Hindawi
Advances in Polymer Technology
Volume 2020, Article ID 9261378, 8 pages
https://doi.org/10.1155/2020/9261378

Research Article

Loading of Iron (II, III) Oxide Nanoparticles in Cryogels Based on Microfibrillar Cellulose for Heavy Metal Ion Separation

Jinhua Yan,[1] **Huanlei Yang**,[1] **Juliana C. da Silva**,[2] **and Orlando J. Rojas**[3]

[1]*Guangdong Industry Polytechnic, Guangzhou 510300, China*
[2]*Department of Forest Sciences, Universidade Federal de Viçosa, Viçosa, Brazil*
[3]*Bio-Based Colloids and Materials, Department of Bioproducts and Biosystems, Aalto University, Vuorimiehentie 1, Espoo 02150, Finland*

Correspondence should be addressed to Jinhua Yan; jhyan2013@163.com

Received 30 May 2019; Accepted 28 July 2019; Published 3 March 2020

Academic Editor: Mingzhi Huang

Cryogels based on microfibrillar cellulose (MFC) and reinforced with chitosan to endow water resistance were loaded with magnetite nanoparticles (MNPs) and characterized by TEM, XRD, and TGA. The MNP-loaded cryogels were tested for heavy metal ion removal from aqueous matrices. The adsorption capacity under equilibrium conditions for Cr(VI), Pd(II), Cd(II), and Zn(II) was measured to be 2755, 2155, 3015, and 4100 mg/g, respectively. The results indicate the potential of the introduced bicomponent cryogels for nanoparticle loading, leading to a remarkably high metal ion sorption capacity.

1. Introduction

Magnetic nanoparticles have been a topic of interest in a wide range of applications, including catalysis [1, 2], biotechnology/biomedicine [3], and environmental remediation [4, 5]. In most of the envisaged applications, the particles perform best when their sizes are below a critical value, typically around 10–20 nm. In such a case, the nanoparticles are a single magnetic domain and show superparamagnetic behavior at temperatures above the so-called blocking temperature [6].

Among the wide variety of magnetic materials that can be prepared in the form of nanoparticles, iron oxides have been considered the most intensive one while being safe. In addition, iron oxide (magnetite) nanoparticles can be easily prepared through coprecipitation of iron salts in alkaline aqueous solutions in the presence of stabilizers [7]. Such coprecipitation is also a convenient way to synthesize iron oxides (either Fe_3O_4 or γ-Fe_2O_3) from aqueous Fe^{2+}/Fe^{3+} salt solutions by the addition of a base under the inert atmosphere at room or elevated temperatures. Using proper stabilizing agents with carboxylate or hydroxyl carboxylate groups, it is possible to produce monodispersed iron oxide magnetic nanoparticles. Moreover, surface complexes readily form between Fe^{2+}/Fe^{3+} and the stabilizing agent, undergoing nucleation and crystal growth, favoring the formation of small units, and preventing aggregation.

Micro/nanofibrillar cellulose (MFC) is isolated from natural cellulose fibers by mechanical action after optional enzymatic or chemical pretreatment. MFC's high aspect ratio, biocompatibility, and abundant active hydroxyl and carboxyl groups make it attractive for applications as a host for particles [8, 9], such as silica [10], silver [11], magnetic [12], and drug [13] nanoparticles. The respective preparation can be carried out in the slurry form, which implies a relatively large usage of water to remove loosely bound reactants and particles. Moreover, since associated reactions occur in the system, with typical high surface areas, large reactant amounts are consumed.

An alternative typical MFC reparation, MFC cryogel, has proven particularly useful in applications where biocompatibility and biodegradability are needed. The cryogels are porous materials of interconnected nanostructures made from precursor hydrogels after replacing the liquid by the gas phase [14]. The unique properties associated with cryogels have led to a wide range of applications such as in

catalysts [15] and as a reaction support [16], as super thermal and sound insulators [17, 19], and as electronics, filters, and storage media, for example, gases in fuel cells [20]. For nanoparticle stabilization and size control, MFC porous materials are very effective as hosts [21, 22]. In the reduction reaction of metal ions, the small pores have been used as sites for nucleation and growth, thus restricting the particle size. Moreover, the resultant hybrid materials have some advantages if given functionalities of the matrix are transferred to the nanoparticles [14]. Here, we propose MFC cryogels for direct use as templates for the preparation of magnetic nanoparticles.

We firstly report a facile method to prepare magnetic nanoparticles and their loading in MFC cryogels followed by a demonstration of their application. The wet strength of the cryogels was improved with the addition of chitosan, and magnetic nanoparticles were successfully synthesized in such a bicomponent system. The hybrid cryogels were shown to be effective in heavy metal ion separation, including Cr(VI), Pb(II), Cd(II), and Zn(II).

2. Experimental

2.1. MFC Preparation. Fully bleached eucalyptus fibers were processed with a microgrinder (x6 passes) at a concentration of 2.3%, producing an MFC suspension, which was kept under refrigeration until further use. The acidic group content of MFC was measured by conductive titration using 0.01 M NaOH, which was added dropwise until the conductivity of the system displayed no further drop. The amount of NaOH consumed was used to calculate the acidic group content [23], calculated to be 70 μmol/g.

2.2. Chitosan and MFC Cryogel Synthesis. Chitosan (MW 10253) was purchased from Aldrich (degree of deacetylation ~85%). Chitosan solutions were prepared by dissolving chitosan (2% by weight) in 1% (by volume) aqueous acetic acid solution [24]. The solution was sonicated for 30 min before use. The MFC suspension was mixed with chitosan at different weight loading ratios, 100/0, 90/10, and 80/20 (MFC/chitosan) as a 0.5% suspension in DI water. High-shear mixing (5 min) was used for this purpose, followed by magnetic bar stirring (3 h) and sonication for another 30 min. Then, the mixture was centrifuged (1.0×10^4 rpm, 0.5 h) to remove excess water. A hydrogel with 3% solid content was thus formed and was frozen with liquid nitrogen. Following this, it was placed in a freeze-dryer (Labconco) for at least 48 h. After water sublimation, the obtained cryogel was characterized (density, strength, and BET surface area). The wet strength was determined qualitatively by immersion and stirring in water for a given time. The BET area of the MFC cryogels was measured before and after MNP loading, after 4 h degassing at 105°C (Gemini VII Series Surface Area Analyzer, Micromeritics Instrument Corporation).

2.2.1. Nanoparticle Loading. The *in situ* loading of magnetic nanoparticles (MNPs) in the cryogels was carried out through the coprecipitation of iron salts of ferrous chloride (Fe^{2+}, 0.05 M) and ferric chloride (Fe^{3+}, 0.1 M) by adding alkaline aqueous solution (0.2 N NaOH) at 60°C. Firstly, the iron solution was prepared by mixing a given volume of 0.05 M Fe^{2+} and 0.1 M Fe^{3+} solutions. The cryogel was loaded with the iron solution dropwise and left undisturbed for 30 min. The iron solution was saturated in the porous cryogel. After air-drying (~1 h), a partially dehydrated matrix was obtained. It was then immersed in 0.2 N NaOH solution at 60°C for 1 h so that the coprecipitation was completed as indicated by no changes in color. The hybrid material was rinsed with Milli-Q water for 1 h to remove water-soluble substances and loosely bound iron particles. Finally, the hybrid material was frozen in liquid nitrogen and freeze-dried. The obtained, magnetic MFC cryogel is thereafter referred to as the MMFC cryogel.

2.3. Cryogel Morphology. The porous structures of the MFC cryogels were examined using a field-emission scanning electron microscope (FESEM) at an accelerating voltage of 20 kV (a JEOL 6400F high-resolution cold field-emission SEM). The MMFC was characterized using a VPSEM (variable-pressure scanning electron microscope (Hitachi S3200N)) with an energy dispersive X-ray spectrometer.

A JEOL 2000FX transmission electron microscope (TEM) operating at 20.0 kV was further utilized for MMFC characterization. For this purpose, a specimen was prepared by cutting the sample into thin slices, using a diamond saw, then cutting 3 mm diameter disks from the slice, thinning the disk on a grinding wheel, dimpling the thinned disk, and then ion milling it to achieve electron transparency.

2.4. Thermal Behavior. In order to determine the thermal decomposition temperature of the hybrid cryogels, a thermogravimetric analysis (TGA) apparatus was used (PerkinElmer TGA Q500), operating with a heating rate of 10°C/min to 500°C in a nitrogen atmosphere. In order to obtain the MNP loading in the cryogel, TGA was performed under oxygen in the T range between 500 and 575°C. The isothermal time at 575°C was 25 min.

2.5. X-Ray Diffraction. MMFC samples were subjected to XRD analysis following 2 theta signals at both small and wide angles to identify iron crystallites. For this purpose, a PANalytical Empyrean X-ray diffractometer was used. The scan range was in 5–40 for small angles, and 10–80 for wide angles.

2.6. Heavy Metal Ion Separation. A stock solution of Cr(VI) (100 mg/L) was prepared by dissolving a certain amount of $K_2Cr_2O_7$ (from Sigma-Aldrich) in 100 mL water obtained from a Millipore™ purification unit. A series of standard metal solutions were prepared by diluting the stock metal solution. A typical adsorption experiment was conducted as follows: 5 mg cryogel was added to a 100 mL Erlenmeyer flask containing 25 mL 100 mg/L Cr(VI) solution and magnetically stirred at 120 rpm for the predetermined time.

The pH of the working solution was maintained at a specified value using 0.01 M NaOH and HCl solutions (both from Sigma-Aldrich). The concentrations of Cr(VI) during adsorption tests were analyzed by spectrophotometry (Agilent 8453 UV-Vis dissolution testing system, Agilent, USA). Pb(II), Cd(II), and Zn(II) solutions were prepared following similar protocols using $Cd(NO_3)_2$, $Pb(NO_3)_2$, and $Zn(NO_3)_2{\cdot}6H_2O$ (Sigma-Aldrich). The uptake capacity of MFC cryogel adsorption Q_e(mg/g) was defined according to the following equation:

$$Q_e = (C_0 - C_e)^* V/m, \quad (1)$$

where C_0 is the metal ion concentration in the initial solution, C_e is the equilibrium concentration (mg/L), V is the volume of metal ion solution (L), and m is the mass of the absorbent material (g).

3. Results and Discussion

3.1. Physical Properties of MMFC Cryogels. The density of the neat MFC cryogel was 0.0258, 0.0505, and 0.0807 g/cm^3, depending on the concentration of the hydrogel precursor of 2, 5, and 8%, respectively. The MFC density was 0.0390 and 0.0395 g/cm^3 upon chitosan loadings of 10 and 20%, respectively, indicating the densification of the system in the presence of the cationic polymer. The MFC and MMFC surface area was measured after 4 h degassing at 105°C (Table 1).

The MFC cryogel with 10% CH loading displayed a higher BET area than that with 20% CH, i.e., chitosan acted as a binder for MFC. In the absence of chitosan, the MFC cryogels were redispersed in water after immersion under magnetic stirring at 610 rpm for 4 h. The cryogels loaded with 10% and 20% chitosan remained intact after immersion, under the same conditions (Figure 1), indicating the reinforcing effect of chitosan.

3.2. MFC and MMFC Morphology. The presence of chitosan produced a denser MFC structure (Figure 2). In the absence of chitosan, the cryogel structure was open, with pores being easily observed (Figure 2(a)). At low chitosan addition (Figure 2(b)), thin "walls" formed between the pores. With the increasing chitosan content to 20% (Figure 2(c)), the thickness of such walls increased. This is because of the characteristic properties of chitosan and its primary amino groups. Besides hydrogen bonding, the reaction between amino and carboxyl groups took place. This reaction has been applied in several cellulose/chitosan hybrid preparations [25–27]. Such chitosan-reinforced MFC cryogels were stable in water.

After MNP loading, the MMFC cryogels exhibited a similar SEM morphology to that before loading. A denser cryogel was relatively tighter, and less capillaries were present, which reduced fluid penetration, resulting in the generation of lower amounts of MNPs. The MNP loading in the MMFC cryogels, as determined by TGA at 575°C in the oxygen atmosphere following 25 min isothermal time, corresponded to 16 and 18%; for MFC cryogels, the chitosan concentration was 10 and 20% (note that an MFC film sample and filter paper yielded 2.8 and 1.8%, respectively).

MMFC samples were subjected to SEM at high magnification (Figure 3). Iron particles were observed on the surface of the fibrils. This was also observed for two other types of cellulose substrates, after the same coprecipitation method, namely, a filter paper and MFC films (see Figure 4). These two substrates showed scattered, monodispersed metal particles but low loadings (Table 2). MFC cryogels comprised abundant, open pores and large BET surface area, offering a good opportunity as a template for iron nanoparticle loading.

Based on the homogeneous particle distribution observed in the SEM images in Figure 3, the MFC cryogel with 20% CH was selected for particle observation under TEM (Figure 4). Both the filter paper and MFC film samples loaded with particles were also observed, as a reference. From the TEM images, the particles were determined to be monodispersed and their size was in the nanoscale. MMFC retained more iron than both the paper and MFC films; the iron particles in such a case were larger and clustered.

3.3. XRD Analysis. An X-ray diffractometer was used to characterize the microstructural and crystallographic features of the iron particles in MMFC (see the XRD pattern at a small angle in Figure 5(a)). MMFC displayed an intense signal at $2\theta = 35.28^\circ$, corresponding to pure Fe_3O_4 crystals (Fe_3O_4 is identified at 35°), confirming their presence. Wide-angle scanning showed similar results to that at small angles (Figure 5(b)). The observed broadness and lower intensity of the profiles indicate a lower degree of crystallinity of Fe_3O_4 particles imbedded in the cellulose matrix.

3.4. Thermal Gravimetric Analysis. In view of the importance of thermal stability in many MMFC applications, we examined the thermal decomposition of the MMFC cryogels by thermogravimetry in the nitrogen atmosphere until 500°C (Figure 6). All TGA curves showed small weight losses below 150°C, from evaporation of the adsorbed moisture. Under nitrogen, the decomposition behavior of MFC was nearly the same at different chitosan loadings. The TGA for MMFC indicated a decomposition temperature from 264 to 318°C. MNPs weakened the substrate thermal stability. The isothermal run (25 min at 575°C) was used to determine the residual mass (MNP amount) in MMFC (TGA under oxygen was run in the 500–575°C range; Table 2).

3.5. Heavy Metal Ion Separation. MFC cryogels were expected to result in partial degradation in acidic solutions at long contact time and high temperature. If the pH of the adsorption solution is lowered, the metal ion separation is maximized. The metal adsorption experiments were conducted under the near-neutral condition at pH 6. Different contact time and initial concentrations were tested for four metal ions: Cr(VI), Pb(II), Cd(II), and Zn(II). Figure 7 shows the removal rate as a function of the contact time and initial ion concentration.

Table 1: BET data for MMFC.

Cryogel BET (m^2/g)	CH 10% (iron loaded)	CH 20% (iron loaded)	CH 10%	CH 20%	CH 30%
MFC/CH	5.4	32.3	24.4	23.5	9.7

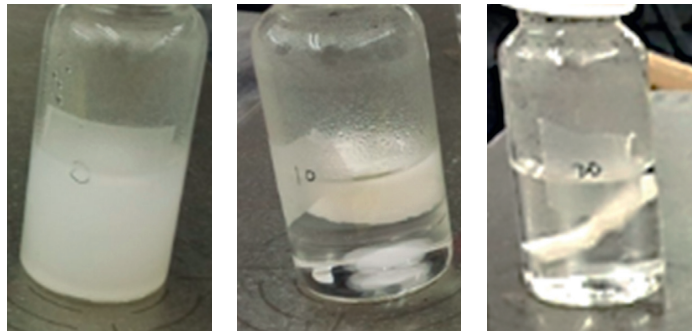

(a) (b) (c)

Figure 1: Cryogels produced from MFC and chitosan and their stability in water at loadings of chitosan (CH) of 0% (a), 10% (b), and 20% (c).

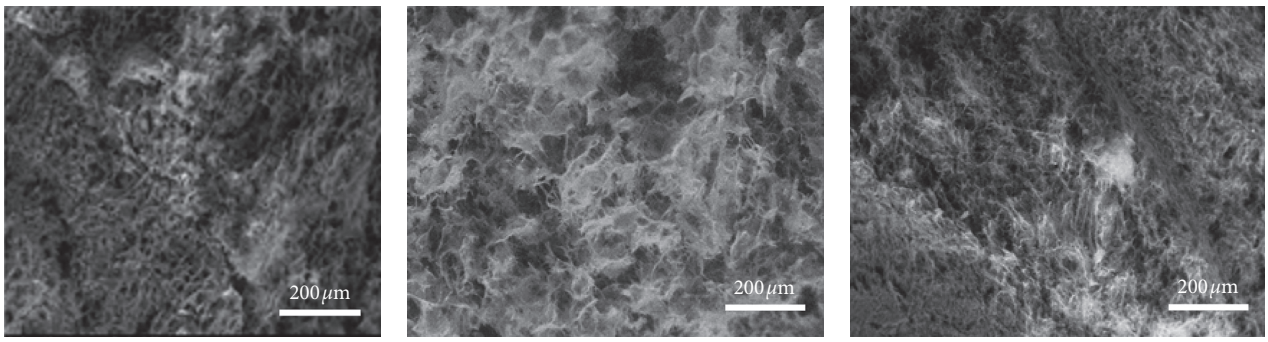

(a) (b) (c)

Figure 2: SEM images of MFC cryogels loaded with chitosan (CH) of 0% (a), 10% (b), and 20% (c).

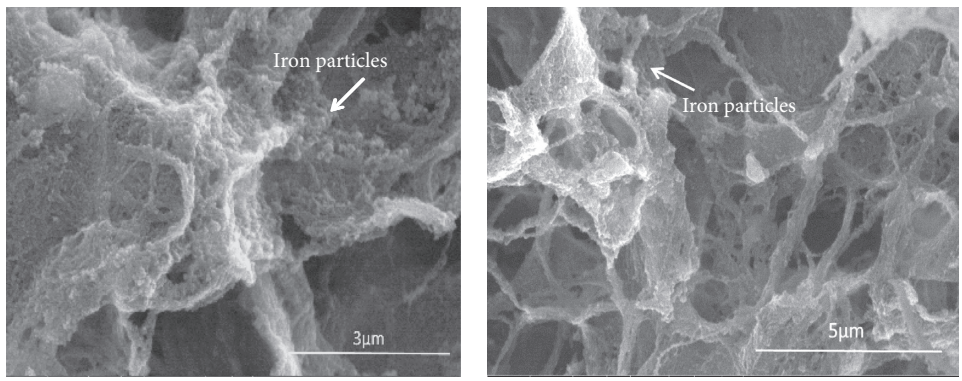

(a) (b)

Figure 3: Iron nanoparticles in MMFC cryogels.

In Figure 7(a), the four ion types showed a similar trend. During the first 20 min contact time, the removal rate reached a maximum adsorption. At longer contact times, the removal rate remained the same. The MMFC could quickly absorb the metal ions. Cr(VI), Pb(II), Cd(II), and Zn(II) presented different removal extent (Figures 7 and 8). Cd(II) and Zn(II) adsorbed more readily than Cr(VI) and Pb(II). The most effective separation corresponded to Cd(II), for a

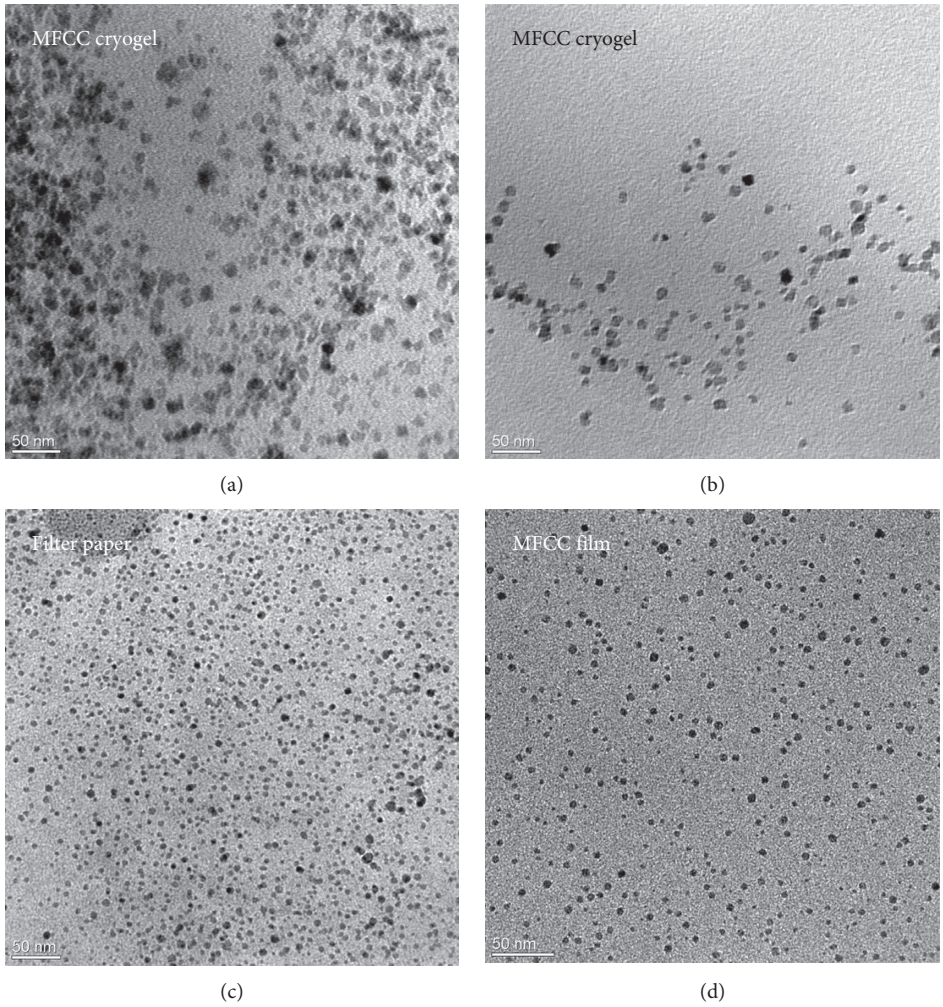

Figure 4: TEM images of the MMFC cryogel and filter paper/MFC film with MNPs (note that the filter paper was treated three times for iron coprecipitation).

Table 2: MNP loading in MFC cryogels (10 and 20% chitosan (CH)), filter paper, and MFC films calculated based on residue mass (TGA, 575°C) per dry sample mass.

CH 10%	CH 20%	Filter paper	MFC film
16%	18.2%	1.8%	2.8%

removal >95% (Cr(VI) and Pb(II) showed removal % close to 52%).

The initial concentration is an important factor in metal ion separation. The 50–1000 mg/L concentration range was adsorbed by MMFC at 60 min contact time, which is long enough for adsorption. The removal % is shown in Figure 7(b). MMFC maintained a high adsorption capacity for all initial concentration, with linear profiles except for Pd^{2+} and Cd(II). The Pd^{2+} removal rate was lowered, from 57% to 43%, and Cd(II) lowered from 95% to 55%. The results indicate that MMFC is a suitable material to remove heavy metal ions from aqueous solution.

In order to express MMFC adsorption capacity, the equilibrium absorption amount Q_e was calculated using equation (1). Figure 8 shows the results for different initial concentrations of the respective metal ion. Four near linear profiles are presented and indicate a high capacity for metal ion removal. The adsorbents were not saturated in solution. Cr(VI), Pd^{2+}, Cd(II), and Zn(II) equilibrium removal amounts were 2755, 2155, 3015, and 4100 mg/g, respectively. The values exceed those reported previously [28–34]. The maximum adsorption capacity of Cr(VI) by the quaternary ammonium-modified NFC cryogel was 18 mg/g, showing 16% removal rate increase compared with nonmodified NFC cryogels [28]. An amino-functionalized magnetic cellulose nanocomposite, used as a Cr(VI) adsorbent, indicated a 171.5 mg/g adsorption amount for 50% magnetic particle ratio to cellulose at pH 2 which decreased rapidly to 60.0 mg/g at pH 6 [29]. Ethylenediamine- and methyl methacrylate-modified NFC cryogels achieved 377 mg/g Cr(VI) adsorption at pH = 2 which decreased below 200 mg/g at pH = 6 [30].

Using cellulose nanocrystals (CNCs) and Fe_2O_3 composite as a Pd^{2+} absorbent, the maximum capacity was measured to be 3.6 mg/g, but 3.3 mg/g for Fe_2O_3 CNC [31].

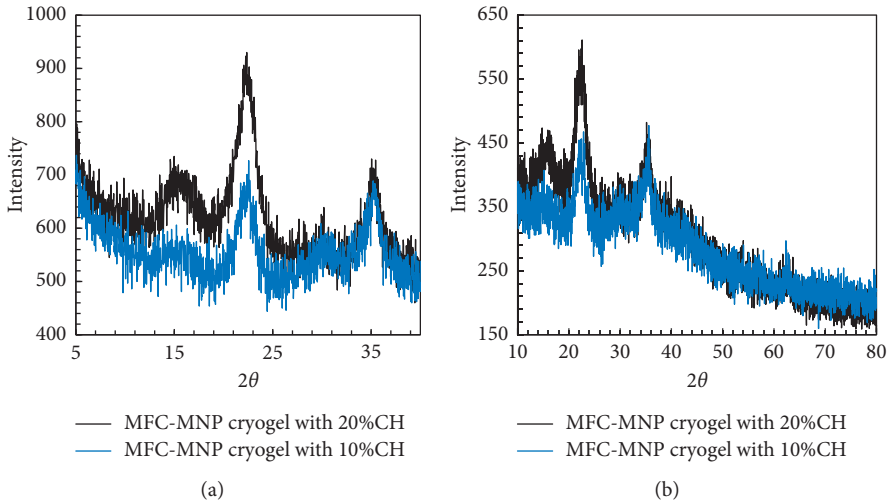

Figure 5: XRD patterns of MMFC cryogels at small (a) and wide (b) angles.

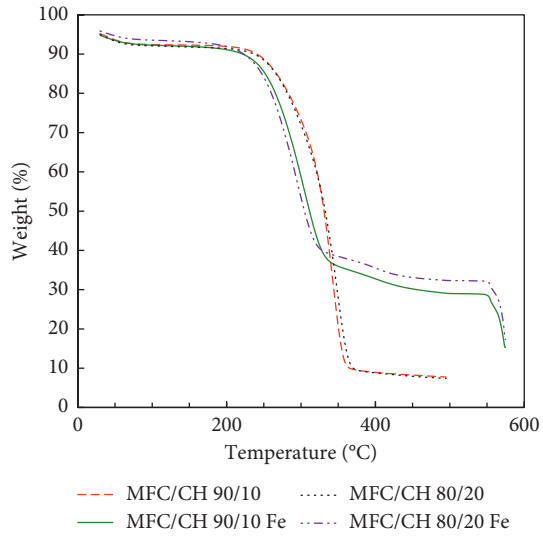

Figure 6: TGA profiles of MFC cryogels with and without MNP loading (under the N_2 atmosphere until 500°C and then under oxygen until 575°C).

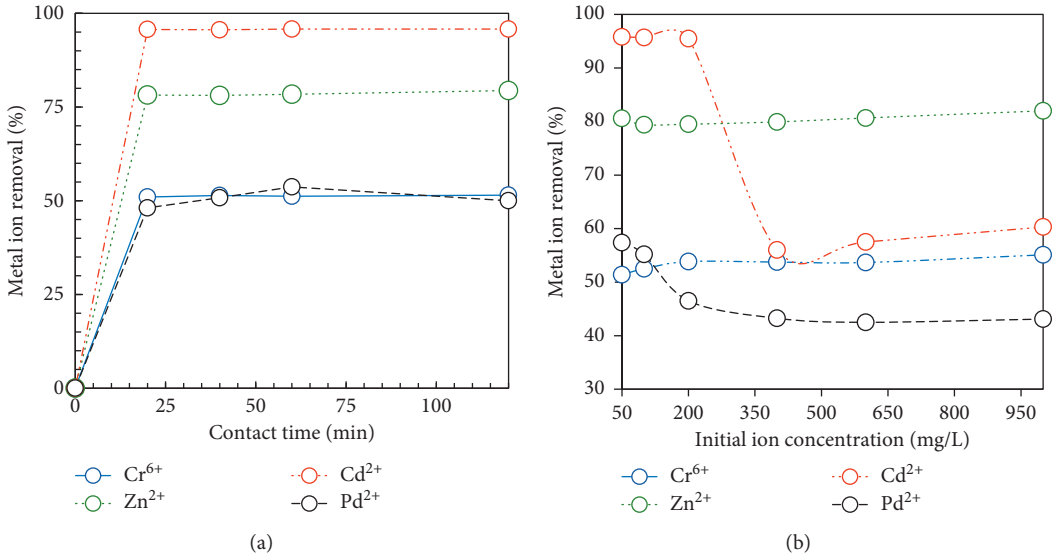

Figure 7: Metal ion removal (%) as a function of the (a) contact time (initial concentration 100 mg/L, pH 6, room temperature, 25 mL solution, 5 mg MMFC) and (b) initial ion concentration (contact time 60 min, pH 6, room temperature, 25 mL solution, 5 mg MMFC). The lines are added as guides to the eye.

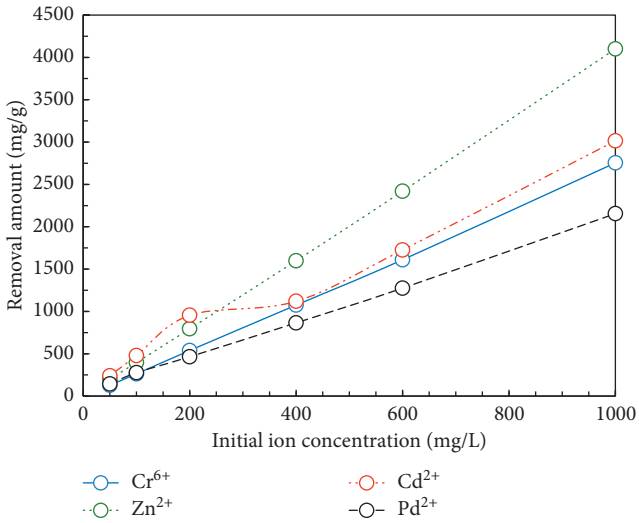

Figure 8: Removal amount (mg/g) relative to the initial ion concentration of Cr(VI), Pd(II), Cd(II), and Zn(II).

Aldehyde-functionalized NFC cryogels showed an improved Pb(II) adsorption of 156 mg/g [32]. Chitosan-based magnetic hydrogel beads reached 171 mg/g Pd^{2+} adsorption capacity with Fe_2O_3 and NFC addition, but only 118 mg/g with no addition [33]. Yu et al. [34] reported that carboxylation of CNC with succinic anhydride resulted in a sorbent with a very high maximum adsorption uptake for Pb(II) (458 mg/g) and Cd(II) (335 mg/g). A Cd(II) adsorption of 3.2 mg/g was reported for CNC and Fe_2O_3 composite adsorbents [31]. Grafting carboxylic groups to chitosan improved the Zn(II) removal from 168 mg/g to 290 mg/g [35]. Amino-functionalized microfibrillated cellulose with the maximum uptake capacity of 388 mg/g was measured for Cd(II) [36]. According to the recent review of nanocellulose-based materials for water purification [37], the MFC/NFC absorbent exhibited a high uptake amount, as high as that of MMFC used in this study.

4. Conclusions

We successfully utilized chitosan to reinforce MFC, producing relatively dense cryogels. MNPs were loaded *in situ* to the reinforced MFC cryogels. The metal-loaded cryogels (MMFC cryogels) displayed monodispersed nanoparticles (TEM and XRD). MMFC cryogels had a good thermal stability (TGA). MMFC cryogels were tested for heavy metal ion separation and separation capacity. The Cr(VI), Pd^{2+}, Cd(II), and Zn(II) equilibrium removal amount corresponded to 2755, 2155, 3015, and 4100 mg/g, respectively. These values for MFC cryogels as metal ion separators indicate an excellent potential for nanoparticle-loaded adsorbents from aqueous solution.

Data Availability

The data used to support the findings of this study are available from the corresponding author upon request.

Conflicts of Interest

The authors declare no conflicts of interest.

Acknowledgments

Xijiang Innovation Team Plan 2016 is greatly acknowledged for support.

References

[1] A.-H. Lu, W. Schmidt, N. Matoussevitch et al., "Nanoengineering of a magnetically separable hydrogenation catalyst," *Angewandte Chemie International Edition*, vol. 43, no. 33, pp. 4303–4306, 2004.

[2] S. C. Tsang, V. r. Caps, I. Paraskevas, D. Chadwick, and D. Thompsett, "Magnetically separable, carbon-supported nanocatalysts for the manufacture of fine chemicals," *Angewandte Chemie International Edition*, vol. 43, no. 42, pp. 5645–5649, 2004.

[3] A. K. Gupta and M. Gupta, "Synthesis and surface engineering of iron oxide nanoparticles for biomedical applications," *Biomaterials*, vol. 26, no. 18, pp. 3995–4021, 2005.

[4] D. W. Elliott and W.-X. Zhang, "Field assessment of nanoscale bimetallic particles for groundwater treatment," *Environmental Science & Technology*, vol. 35, no. 24, pp. 4922–4926, 2001.

[5] M. Takafuji, S. Ide, H. Ihara, and Z. Xu, "Preparation of poly(1-vinylimidazole)-grafted magnetic nanoparticles and their application for removal of metal ions," *Chemistry of Materials*, vol. 16, no. 10, pp. 1977–1983, 2004.

[6] A.-H. Lu, E. L. Salabas, and F. Schüth, "Magnetic nanoparticles: synthesis, protection, functionalization, and application," *Angewandte Chemie International Edition*, vol. 46, no. 8, pp. 1222–1244, 2007.

[7] A. Ditsch, P. E. Laibinis, D. I. C. Wang, and T. A. Hatton, "Controlled clustering and enhanced stability of polymer-coated magnetic nanoparticles," *Langmuir*, vol. 21, no. 13, pp. 6006–6018, 2005.

[8] F. Hoeng, A. Denneulin, and J. Bras, "Use of nanocellulose in printed electronics: a review," *Nanoscale*, vol. 8, no. 27, pp. 13131–13154, 2016.

[9] H. Zhang, J. Liu, M. Guan et al., "Nanofibrillated cellulose (NFC) as a pore size mediator in the preparation of thermally resistant separators for lithium ion batteries," *ACS Sustainable Chemistry & Engineering*, vol. 6, no. 4, pp. 4838–4844, 2018.

[10] X. An, Y. Wen, A. Almujil et al., "Nano-fibrillated cellulose (NFC) as versatile carriers of TiO_2 nanoparticles (TNPs) for photocatalytic hydrogen generation," *RSC Advances*, vol. 6, no. 92, pp. 89457–89466, 2016.

[11] H. Dong, J. F. Snyder, D. T. Tran, and J. L. Leadore, "Hydrogel, aerogel and film of cellulose nanofibrils functionalized with silver nanoparticles," *Carbohydrate Polymers*, vol. 95, no. 2, pp. 760–767, 2013.

[12] T. Nypelö, H. Pynnönen, M. Österberg, J. Paltakari, and J. Laine, "Interactions between inorganic nanoparticles and cellulose nanofibrils," *Cellulose*, vol. 19, no. 3, pp. 779–792, 2012.

[13] R. Kolakovic, L. Peltonen, A. Laukkanen, J. Hirvonen, and T. Laaksonen, "Nanofibrillar cellulose films for controlled drug delivery," *European Journal of Pharmaceutics and Biopharmaceutics*, vol. 82, no. 2, pp. 308–315, 2012.

[14] K. J. De France, T. Hoare, and E. D. Cranston, "Review of hydrogels and aerogels containing nanocellulose," *Chemistry of Materials*, vol. 29, no. 11, pp. 4609–4631, 2017.

[15] M. Mukhopadhyay and B. S. Rao, "Modeling of supercritical drying of ethanol-soaked silica aerogels with carbon dioxide," *Journal of Chemical Technology & Biotechnology*, vol. 83, no. 8, pp. 1101–1109, 2008.

[16] J. Gu, C. Hu, W. Zhang, and A. B. Dichiara, "Reagentless preparation of shape memory cellulose nanofibril aerogels decorated with Pd nanoparticles and their application in dye discoloration," *Applied Catalysis B: Environmental*, vol. 237, pp. 482–490, 2018.

[17] C. Jiménez-Saelices, B. Seantier, B. Cathala, and Y. Grohens, "Spray freeze-dried nanofibrillated cellulose aerogels with thermal superinsulating properties," *Carbohydrate Polymers*, vol. 157, pp. 105–113, 2017.

[18] G. Zu, K. Kanamori, T. Shimizu et al., "Versatile double-cross-linking approach to transparent, machinable, super-compressible, highly bendable aerogel thermal super-insulators," *Chemistry of Materials*, vol. 30, no. 8, pp. 2759–2770, 2018.

[19] R. Baetens, B. P. Jelle, and A. Gustavsen, "Aerogel insulation for building applications: a state-of-the-art review," *Energy and Buildings*, vol. 43, no. 4, pp. 761–769, 2011.

[20] G. Nyström, A. Marais, E. Karabulut, L. Wågberg, Y. Cui, and M. M. Hamedi, "Self-assembled three-dimensional and compressible interdigitated thin-film supercapacitors and batteries," *Nature Communications*, vol. 6, p. 7259, 2015.

[21] J. Cai, S. Kimura, M. Wada, and S. Kuga, "Nanoporous cellulose as metal nanoparticles support," *Biomacromolecules*, vol. 10, no. 1, pp. 87–94, 2009.

[22] S. Liu, Q. Yan, D. Tao, T. Yu, and X. Liu, "Highly flexible magnetic composite aerogels prepared by using cellulose nanofibril networks as templates," *Carbohydrate Polymers*, vol. 89, no. 2, pp. 551–557, 2012.

[23] SCAN-CM 65:02, Pulp Total acidic group content, Conductometric titration method.

[24] C. M. F. Susana, L. Oliveira, C. S. R. Freire et al., "Novel transparent nanocomposite films based on chitosan and bacterial cellulose," *Green Chemistry*, vol. 11, pp. 2023–2029, 2009.

[25] Z. Li, L. Shao, W. Hu et al., "Excellent reusable chitosan/cellulose aerogel as an oil and organic solvent absorbent," *Carbohydrate Polymers*, vol. 191, pp. 183–190, 2018.

[26] H. Yang, A. Sheikhi, and T. G. M. van de Ven, "Reusable green aerogels from cross-linked hairy nanocrystalline cellulose and modified chitosan for dye removal," *Langmuir*, vol. 32, no. 45, pp. 11771–11779, 2016.

[27] G. Meng, H. Peng, J. Wu et al., "Fabrication of super-hydrophobic cellulose/chitosan composite aerogel for oil/water separation," *Fibers and Polymers*, vol. 18, no. 4, pp. 706–712, 2017.

[28] X. He, L. Cheng, Y. Wang, J. Zhao, W. Zhang, and C. Lu, "Aerogels from quaternary ammonium-functionalized cellulose nanofibers for rapid removal of Cr(VI) from water," *Carbohydrate Polymers*, vol. 111, pp. 683–687, 2014.

[29] X. Sun, L. Yang, Q. Li et al., "Amino-functionalized magnetic cellulose nanocomposite as adsorbent for removal of Cr(VI): synthesis and adsorption studies," *Chemical Engineering Journal*, vol. 241, pp. 175–183, 2014.

[30] J. Q. Zhao, X. F. Zhang, X. He, M. J. Xiao, W. Zhang, and C. H. Lu, "A super biosorbent from dendrimer poly(amido-amine)-grafted cellulose nanofibril aerogels for effective removal of Cr(VI)," *Journal of Materials Chemistry A*, vol. 3, no. 28, pp. 14703–14711, 2015.

[31] H. Liu, *Synthesis and Application of Cellulose Nanocrystals and Its Nano-Composites*, Chinese Forestry Institute, Beijng, China, 2011.

[32] C. Yao, F. Wang, Z. Cai, and X. Wang, "Aldehyde-functionalized porous nanocellulose for effective removal of heavy metal ions from aqueous solutions," *RSC Advances*, vol. 6, no. 95, pp. 92648–92654, 2016.

[33] Y. Zhou, S. Fu, L. Zhang, H. Zhan, and M. V. Levit, "Use of carboxylated cellulose nanofibrils-filled magnetic chitosan hydrogel beads as adsorbents for Pb(II)," *Carbohydrate Polymers*, vol. 101, pp. 75–82, 2014.

[34] X. Yu, S. Tong, M. Ge et al., "Adsorption of heavy metal ions from aqueous solution by carboxylated cellulose nanocrystals," *Journal of Environmental Sciences*, vol. 25, no. 5, pp. 933–943, 2013.

[35] G. Z. Kyzas, P. I. Siafaka, E. G. Pavlidou, K. J. Chrissafis, and D. N. Bikiaris, "Synthesis and adsorption application of succinyl-grafted chitosan for the simultaneous removal of zinc and cationic dye from binary hazardous mixtures," *Chemical Engineering Journal*, vol. 259, pp. 438–448, 2015.

[36] S. Hokkanen, E. Repo, T. Suopajärvi, H. Liimatainen, J. Niinimaa, and M. Sillanpää, "Adsorption of Ni(II), Cu(II) and Cd(II) from aqueous solutions by amino modified nanostructured microfibrillated cellulose," *Cellulose*, vol. 21, no. 3, pp. 1471–1487, 2014.

[37] H. Voisin, L. Bergström, P. Liu, and A. P. Mathew, "Nanocellulose-based materials for water purification," *Nanomaterials*, vol. 7, p. 57, 2017.